Draft version November 12, 2013
Preprint typeset using LaTeX style emulateapj v. 08/22/09

MAGNETIC HELICITY AND ENERGY SPECTRA OF A SOLAR ACTIVE REGION

Hongqi Zhang[1], Axel Brandenburg[2,3] and D.D. Sokoloff[4,5]
[1]Key Laboratory of Solar Activity, National Astronomical Observatories, Chinese Academy of Sciences, Beijing 100012, China
[2]Nordita, KTH Royal Institute of Technology and Stockholm University, Roslagstullsbacken 23, 10691 Stockholm, Sweden
[3]Department of Astronomy, AlbaNova University Center, Stockholm University, 10691 Stockholm, Sweden
[4]Department of Physics, Moscow University, 119992 Moscow, Russia
[5]Pushkov Institute of Terrestrial Magnetism, Ionosphere and Radiowave Propagation of the Russian Academy of Sciences, Troitsk, Moscow, 142190, Russia

Draft version November 12, 2013

ABSTRACT

We compute magnetic helicity and energy spectra of the solar active region NOAA 11158 during 11–15 February 2011 at 20° southern heliographic latitude using observational photospheric vector magnetograms. We adopt the isotropic representation of the Fourier-transformed two-point correlation tensor of the magnetic field. The sign of magnetic helicity turns out to be predominantly positive at all wavenumbers. This sign is consistent with what is theoretically expected for the southern hemisphere. The relative magnetic helicity is around 8% and strongest at intermediate wavenumbers of $k \approx 0.4\,\mathrm{Mm}^{-1}$, corresponding to a scale of $2\pi/k \approx 16\,\mathrm{Mm}$. The same sign and a somewhat smaller value is also found for the relative current helicity evaluated in real space based on the vertical components of magnetic field and current density. The current helicity spectrum is estimated from the magnetic helicity spectrum and its modulus shows a $k^{-5/3}$ spectrum at large wavenumbers. A similar power law is also obtained for the magnetic energy spectrum. The comparison of energy spectra evaluated separately from the horizontal and vertical fields agree for wavenumbers below $3\,\mathrm{Mm}^{-1}$, corresponding to scales above 2 Mm. This gives some justification to our assumption of isotropy and places limits resulting from instrumental artefacts at small scales.

Subject headings: Sun: activity—Sun: magnetic topology—Sun: photosphere—Sun: dynamo

1. INTRODUCTION

Magnetic helicity is an important quantity that reflects the topology of the magnetic field (Woltjer, 1958a,b and Taylor, 1986). Pioneering studies of magnetic helicity in solar physics have been done by several authors focussing on the accumulation of magnetic helicity in the solar atmosphere (e.g. Berger 1984; Chae 2001), the force-free α coefficient, and the mean current helicity density in solar active regions (Seehafer 1990).

Besides the hemispheric sign distribution of large-scale helical features in active regions (Pevtsov et al. 1994; Abramenko et al. 1997), there can be patches of positive and negative helicities intermixed in a mesh-like pattern in the sunspot umbra and a threaded pattern in the sunspot penumbra (Su et al. 2009). Zhang (2010) showed that the individual magnetic fibrils tend to be dominated by the current density component caused by magnetic inhomogeneity, while the large-scale magnetic region tends to be dominated by the component of the current density associated with the magnetic twist. Venkatakrishnan & Tiwari (2009) pointed out that the existence of a global twist for a sunspot – even in the absence of a net current – is consistent with a fibril structure of sunspot magnetic fields.

The redistribution of magnetic helicity contained within different scales was argued to be the interchange of twist and writhe due to magnetic helicity conservation (cf. Zeldovich et al. 1983; Kerr & Brandenburg 1999). Furthermore, the spectral magnetic helicity distribution is important for understanding the operation of the solar dynamo (Brandenburg & Subramanian 2005a). It has been argued that, if the large-scale magnetic field is generated by an α effect (Krause & Rädler 1980), it must produce magnetic helicity of opposite signs at large and small length scales (Seehafer 1996; Ji 1999). We call such a magnetic field bi-helical (Yousef & Brandenburg 2003). To alleviate the possibility of catastrophic (magnetic Reynolds number-dependent) quenching of the α effect (Gruzinov & Diamond 1994) and slow saturation (Brandenburg 2001), one must invoke magnetic helicity fluxes from small-scale magnetic fields (Kleeorin et al. 2000; Blackman & Field 2000; Brandenburg & Subramanian 2005a; Brandenburg et al. 2009; Hubbard & Brandenburg 2012). Direct evidence for the existence of a bi-helical magnetic field has come recently from measurements in the solar wind (Brandenburg et al. 2011) and from numerical simulations of plasmoid ejections above the surface of a dynamo (Warnecke et al. 2011, 2012).

In the present paper, we determine the spectrum of magnetic helicity and its relationship with magnetic energy from photospheric vector magnetograms of a solar active region. We use a technique that is based on the spectral representation of the magnetic two-point correlation tensor. It is related to the method of Matthaeus et al. (1982) for determining the magnetic helicity spectrum from in situ measurements of the magnetic field in the solar wind. It has recently been applied to data from *Ulysses* to show that the magnetic field at high heliographic latitudes has opposite signs of magnetic helicity in the two hemispheres and also at large and small length scales (Brandenburg et al. 2011).

2. DATA ANALYSIS

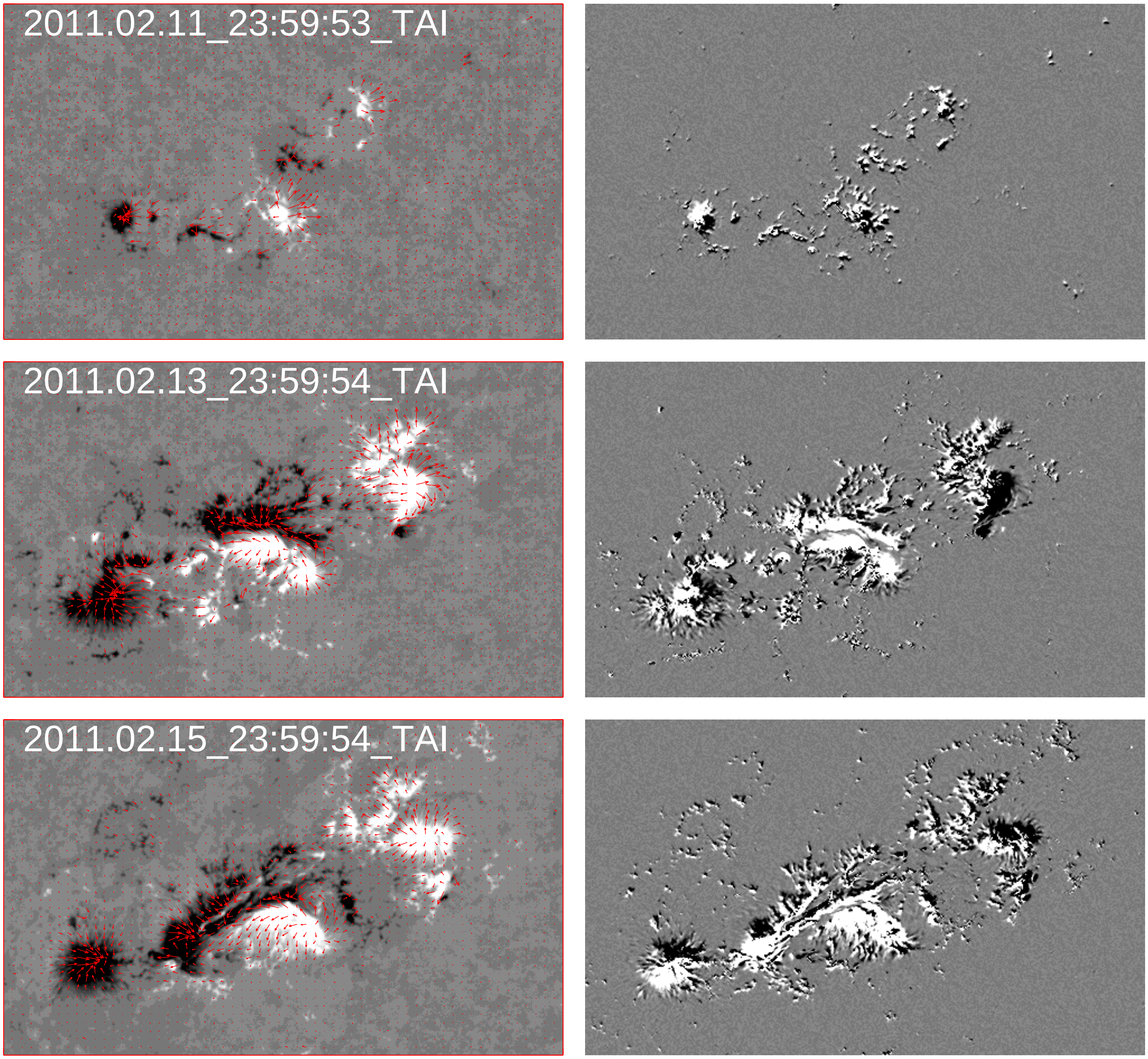

FIG. 1.— Photospheric vector magnetograms (left) and plots of J_zB_z (right) for the active region NOAA 11158 between 11–15 February 2011. The arrows show the transverse component of the magnetic field. Light (dark) shades indicate positive (negative) values of B_z on the left and J_zB_z on the right.

We have analyzed data from the solar active region NOAA 11158 during 11–15 February 2011, taken by the Helioseismic and Magnetic Imager (HMI) on board the *Solar Dynamics Observatory* (SDO). The pixel resolution of magnetogram is about $0.5''$, and the field of view is $250'' \times 150''$. Figure 1 shows photospheric vector magnetograms (left) and the corresponding distribution of $h_C^{(z)} = J_zB_z$ (right) from the vector magnetograms of that active region on different days. Here, $J_z = \partial B_y/\partial x - \partial B_x/\partial y$ is proportional to the vertical component of the current density. The superscript '(z)' on $h_C^{(z)}$ indicates that only the vertical contribution to the current helicity density is available.

Through direct inspection of the vector magnetograms it is evident that there tends to be a counterclockwise (clockwise) swirl of the horizontal magnetic field in regions where the vertical field component points upward (downward). This suggests that the magnetic field has positive helicity. Indeed, the mean value of the current helicity density, $\mathcal{H}_C^{(z)} = \langle h_C^{(z)} \rangle$, is positive and $\approx 2.7\,\mathrm{G}^2\,\mathrm{km}^{-1}$. Furthermore, as a proxy of the force-free α parameter, we determine $\alpha = J_z/B_z$, which is on the average $\langle \alpha \rangle \approx 2.8 \times 10^{-5}\,\mathrm{km}^{-1}$. To estimate the relative current helicity, we consider the ratio

$$r_C = \langle J_zB_z \rangle \Big/ \left(\langle J_z^2 \rangle \langle B_z^2 \rangle \right)^{1/2}. \tag{1}$$

For the active region NOAA 11158 we find $r_C = +0.034$.

Let us now turn to the two-point correlation tensor, $B_i(\boldsymbol{x},t), B_j(\boldsymbol{x}+\boldsymbol{\xi},t)$, where $\boldsymbol{x}$ is the position vector on the two-dimensional surface. Its Fourier transform with respect to $\boldsymbol{\xi}$ can be written as

$$\left\langle \hat{B}_i(\boldsymbol{k},t)\hat{B}_j^*(\boldsymbol{k}',t)\right\rangle = \Gamma_{ij}(\boldsymbol{k},t)\delta^2(\boldsymbol{k}-\boldsymbol{k}'), \tag{2}$$

where $\hat{B}_i(\boldsymbol{k},t) = \int B_i(\boldsymbol{x},t)\,e^{i\boldsymbol{k}\cdot\boldsymbol{x}}d^2x$ is the two-dimensional Fourier transform, the subscript i refers to one of the three magnetic field components, and the asterisk denotes complex conjugation. Under isotropic conditions, the spectral correlation tensor $\Gamma_{ij}(\boldsymbol{k},t)$ takes the form (cf. Moffatt 1978)

$$\Gamma_{ij}(\boldsymbol{k},t) = \frac{2E_M(k,t)}{4\pi k}(\delta_{ij}-\hat{k}_i\hat{k}_j)+\frac{iH_M(k,t)}{4\pi k}\varepsilon_{ijk}k_k, \tag{3}$$

where $\hat{k}_i = k_i/k$ is a component of the unit vector of $\boldsymbol{k}$, $k=|\boldsymbol{k}|$ is its modulus with $k^2=k_x^2+k_y^2$, and $E_M(k,t)$ and $H_M(k,t)$ are the magnetic energy and magnetic helicity spectra, normalized such that

$$\mathcal{E}_M(t) \equiv \frac{1}{2}\langle \boldsymbol{B}^2\rangle = \int_0^\infty E_M(k,t)\,dk,$$

$$\mathcal{H}_M(t) \equiv \langle \boldsymbol{A}\cdot\boldsymbol{B}\rangle = \int_0^\infty H_M(k,t)\,dk. \tag{4}$$

We emphasize that the expression for $\Gamma_{ij}(\boldsymbol{k},t)$ differs from that of Moffatt (1978) by a factor $2k$, because we are here in two dimensions, so the differential for the integration over shells in wavenumber space changes from $4\pi k^2\,dk$ to $2\pi k\,dk$.

Note that the magnetic vector potential is not an observable quantity, so the magnetic helicity might not be gauge-invariant. However, if the spatial average is over all space, or if the magnetic field falls off sufficiently rapidly toward the boundaries, both $\mathcal{H}_M(t)$ and $H_M(k,t)$ are gauge-invariant. Indeed, with the present analysis, $H_M(k,t)$ is manifestly gauge-invariant, because it has been computed directly from the magnetic field as obtained through the photospheric vector magnetogram.

The components of the correlation tensor of turbulent magnetic field can be written in the form

$$4\pi k\boldsymbol{\Gamma}(k,\phi_k) = \tag{5}$$
$$\begin{pmatrix} (1-\cos^2\phi_k)2E_M & -\sin 2\phi_k E_M & -ik\sin\phi_k H_M \\ -\sin 2\phi_k E_M & (1-\sin^2\phi_k)2E_M & ik\cos\phi_k H_M \\ ik\sin\phi_k H_M & -ik\cos\phi_k H_M & 2E_M \end{pmatrix},$$

where we have defined the polar angle in wavenumber space, $\phi_k = \tan^{-1}(k_y,k_x)$, so that $k_x = k\cos\phi_k$ and $k_y = k\sin\phi_k$. For brevity, we have also skipped the arguments k and t on $E_M(k,t)$ and $H_M(k,t)$.

In the following we present shell-integrated spectra. However, because we consider here two-dimensional spectra, they correspond to the power in annuli of radius k and are obtained as

$$2E_M(k) = 2\pi k\,\mathrm{Re}\,\langle\Gamma_{xx}+\Gamma_{yy}+\Gamma_{zz}\rangle_{\phi_k}, \tag{6}$$

$$kH_M(k) = 4\pi k\,\mathrm{Im}\,\langle\cos\phi_k\Gamma_{yz}-\sin\phi_k\Gamma_{xz}\rangle_{\phi_k}, \tag{7}$$

where the angle brackets with subscript ϕ_k denote averaging over annuli in wavenumber space.

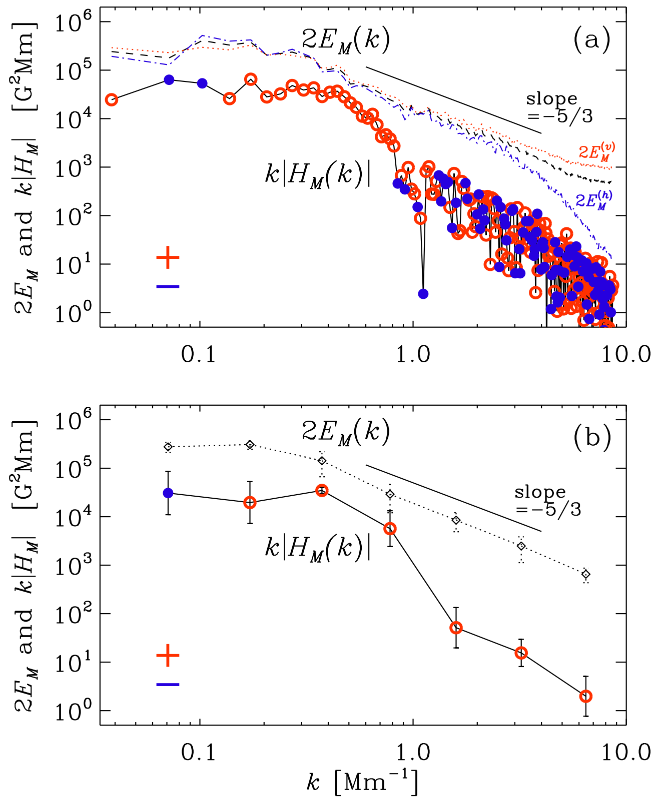

FIG. 2.— (a) $2E_M(k)$ (solid line) and $k|H_M(k)|$ (dotted line). Positive (negative) values of $H_M(k)$ are indicated by open (closed) symbols, respectively. $2E_M^{(h)}(k)$ (red, dotted) and $2E_M^{()}V(k)$ (blue, dash-dotted) are shown for comparison. (b) Same as upper panel, but the magnetic helicity is averaged over broad logarithmically spaced wavenumber bins.

The realizability condition (Moffatt 1969) implies that

$$k|H_M(k,t)| \le 2E_M(k,t). \tag{8}$$

It is therefore convenient to plot $k|H_M(k,t)|$ and $2E_M(k,t)$ on the same graph, which allows one to judge how helical the magnetic field is at each wavenumber. Furthermore, to assess the degree of isotropy, we also consider magnetic energy spectra $E_M^{(h)}(k)$ and $E_M^{(v)}(k)$ based respectively on the horizontal and vertical magnetic field components, defined via

$$2E_M^{(h)}(k) = 4\pi k\,\mathrm{Re}\,\langle\Gamma_{xx}+\Gamma_{yy}\rangle_{\phi_k}, \tag{9}$$

$$2E_M^{(v)}(k) = 4\pi k\,\mathrm{Re}\,\langle\Gamma_{zz}\rangle_{\phi_k}. \tag{10}$$

Under isotropic conditions, we expect $E_M(k) \approx E_M^{(h)}(k) \approx E_M^{(v)}(k)$.

We now consider magnetic energy and helicity spectra for the active region NOAA 11158. The calculated region of the field of view is $256'' \times 256''$ (i.e. 512×512 pixels). We present first the results for NOAA 11158 at 23:59:54UT on 13 February 2011; see Figure 2(a). It turns out that the magnetic energy spectrum has a clear $k^{-5/3}$ range for wavenumbers in the interval $0.5\,\mathrm{Mm}^{-1} < k < 5\,\mathrm{Mm}^{-1}$. The magnetic helicity spectrum is predominantly positive at intermediate wavenumbers, but we also see that toward high wavenumbers the magnetic helicity is fluctuating strongly around small values. To

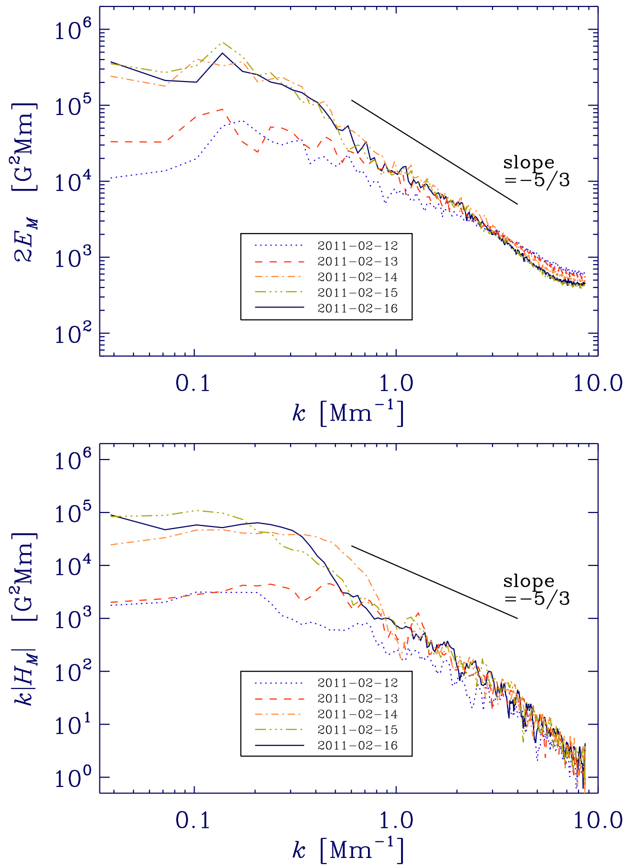

FIG. 3.— Similar to Figure 2, showing $E_M(k,t)$ (upper panel) and $k|H_M(k,t)|$ (lower panel) for the other days.

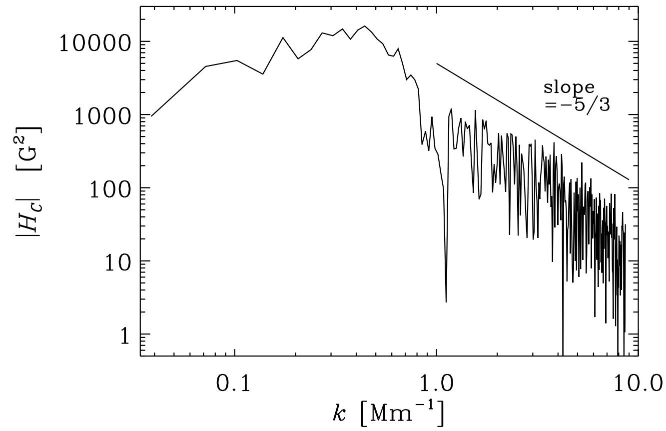

FIG. 4.— Unsigned current helicity spectrum, $|H_C(k)|$.

determine the sign of magnetic helicity at these smaller scales, we average the spectrum over broad, logarithmically spaced wavenumber bins; see the lower panel of Figure 2. This shows that even at smaller length scales the magnetic helicity is still positive, again consistent with the fact that this active region is at southern latitudes.

To calculate the relative magnetic helicity, we define the integral scale of the magnetic field in the usual way as

$$L_M = \int k^{-1} E_M(k)\, dk \bigg/ \int E_M(k)\, dk. \qquad (11)$$

The realizability condition of Equation (8) can be rewritten in the integrated form (e.g. Kahniashvili et al. 2013) as

$$\mathcal{H}_M = \int H_M\, dk \le 2 \int k^{-1} E_M(k)\, dk \equiv 2 L_M \mathcal{E}_M. \quad (12)$$

In particular, we have $|\mathcal{H}_M(t)| \le 2L_M\mathcal{E}_M(t)$. This allows us then to define the relative magnetic helicity,

$$r_M = \mathcal{H}_M / 2L_M\mathcal{E}_M, \qquad (13)$$

which obeys $|r_M| \le 1$. For the active region NOAA 11158 at 23:59:54 UT on 13 February 2011 we have $L_M \approx 5.8\,$Mm, and $r_M \approx 0.083$. The relative magnetic helicity has thus the same sign as the relative current helicity.

Interestingly, the magnetic energy spectra $E_M^{(h)}(k)$ and $E_M^{(v)}(k)$ based respectively on the horizontal and vertical magnetic field components agree remarkably well at wavenumbers below $k = 3\,\mathrm{Mm}^{-1}$, corresponding to length scales larger than 2 Mm. This suggests that our assumption of isotropy might be a reasonable one. The reason for the mutual departure between $E_M^{(h)}(k)$ and $E_M^{(v)}(k)$ at larger wavenumbers might be connected with different accuracies of horizontal and vertical magnetic field measurements (Zhang et al. 2012). Our spectral analysis thus allows us to isolate potential artefacts in the determination of magnetic helicity from photospheric vector magnetograms.

In Figure 3 we show $2E_M(k)$ and $k|H_M(k)|$ for different days. It turns out that on small scales the spectra are rather similar in time, and that there are differences in the amplitude mainly on large scales. Also the sign of $H_M(k)$ remains positive for the different days.

We find that the mean spectral values of magnetic energy of the active region at the solar surface is consistent with a $k^{-5/3}$ power law, which is similar to hydrodynamic turbulence (Kolmogorov, 1941; Obukhov, 1941; Batchelor, 1953). Similar results have been calculated by Abramenko (2005) and Stenflo (2012) for solar magnetic fields.

Under isotropic conditions, the current helicity spectrum, $H_C(k,t)$, is related to the magnetic helicity spectrum via

$$H_C(k,t) \sim k^2 H_M(k,t). \qquad (14)$$

It is normalized such that $\int H_C(k)\, dk = \langle \boldsymbol{J}\cdot\boldsymbol{B}\rangle$. In Figure 4 we show $H_C(k)$ obtained in this way. For $k \gtrsim 1\mathrm{Mm}^{-1}$, the current helicity spectrum shows a $k^{-5/3}$ spectrum, which is consistent with numerical simulations of helically forced hydromagnetic turbulence (Brandenburg and Subramanian 2005b). Similar spectra have also been obtained for the kinetic helicity (André & Lesieur 1977; Borue & Orszag 1997), which implies that the relative helicity decreases toward smaller scales; see the corresponding discussion on p. 286 of Moffatt (1978).

3. CONCLUSIONS

We have applied a novel technique to estimate the magnetic helicity spectrum using vector magnetogram data at the solar surface. We have made use of the assumption that the spectral two-point correlation tensor of the magnetic field can be approximated by its isotropic representation. This assumption is partially justified by the fact that the energy spectra from horizontal and vertical magnetic fields agree at wavenumbers below $2\,\mathrm{Mm}^{-1}$. However, it will be important to assess the assumption of isotropy in future work through comparison with simulations. An example are the simulations of Losada et al. (2013), who employed however only a one-dimensional representation of the spectral two-point correlation function. Nevertheless, the present results look promising, because the sign of magnetic helicity is the same over a broad range of wavenumbers and consistent with that theoretically expected for the southern hemisphere. Except for the smallest wavenumbers, magnetic and current helicities have essentially the same sign. Therefore, a sign change is only expected at smaller wavenumbers corresponding to scales comparable to those of the Sun itself.

It would useful to extend our analysis to a larger surface area of the Sun to see whether there is evidence for a sign change toward small wavenumbers. Figure 2 gives indications of an opposite sign for $k \leq 0.1\,\mathrm{Mm}^{-1}$, which corresponds to scales that are still much smaller than those of the Sun. However, measurements of spectral power on scales comparable to those of the observed magnetogram itself are not sufficiently reliable.

Our results suggest that the unsigned current helicity spectrum shows a $k^{-5/3}$ power law. This is in agreement with simulations of hydromagnetic turbulence (Brandenburg and Subramanian 2005b) and implies that the turbulence becomes progressively less helical toward smaller scales. At a scale of $\approx 6\,\mathrm{Mm}$, the relative magnetic helicity reaches values around 0.08. This magnetic helicity must have its origin in the underlying dynamo process, and can be traced back to the interaction between rotation and stratification. Losada et al. (2013) parameterized these two effects in terms of a stratification parameter Gr and a Coriolis number Co and found that the relative kinetic helicity is approximately 2 Gr Co. For the Sun, they estimate Gr=1/6.5, so a relative helicity of 0.08 might correspond to Co=0.2–0.3. For the solar rotation rate, this corresponds to a correlation time of about 10 hours, which translates to a depth of about 10 Mm. Again, more precise estimates should be obtained using realistic simulations.

In addition to measuring magnetic helicity over larger regions, it will be important to apply our technique to many active regions covering both hemispheres of the Sun and different stages during the solar cycle. This would allow us to verify the expected hemispheric dependence of magnetic helicity. Compared with previous determinations of the hemispheric dependence of current helicity (Zhang et al. 2012), our technique allows us to isolate instrumental artefacts resulting from different resolutions of vector magnetograms for horizontal and vertical magnetic fields.

This study is supported by grants from the National Natural Science Foundation (NNSF) of China under the project grants 10921303, 11221063 and 41174153 (HZ), the NNSF of China and the Russian Foundation for Basic Research under the collaborative China-Russian project 13-02-91158 (HZ+DDS), the European Research Council under the AstroDyn Research Project No. 227952, and the Swedish Research Council under the project grants 2012-5797 and 621-2011-5076 (AB).

REFERENCES

Abramenko, V. I., Wang, T., & Yurchishin, V. B., 1997, SoPh, 174, 291
Abramenko, V. I., 2005, ApJ, 629, 1141
André, J.-C., & Lesieur, M. 1977, JFM, 81, 187
Batchelor, G. K., 1953, An Introduction to Fluid Dynamics, Cambridge University Press
Berger, M. A., & Field, G. B., 1984, JFM 147, 133
Blackman, E. G., & Field, G. B. 2000, ApJ, 534, 984
Borue, V., & Orszag, S. A. 1997, PhRvE, 55, 7005
Brandenburg, A. 2001, ApJ, 550, 824
Brandenburg, A., & Subramanian, K., 2005a, PhR, 417, 1
Brandenburg, A., & Subramanian, K. 2005b, A&A, 439, 835
Brandenburg, A., Candelaresi, S., & Chatterjee, P. 2009, MNRAS, 398, 1414
Brandenburg, A., Subramanian, K., Balogh, A., & Goldstein, M. L. 2011, ApJ, 734, 9
Chae, J., 2001, ApJ, 560, L95
Gruzinov, A. V., & Diamond, P. H. 1994, PhRvL, 72, 1651
Ji, H. 1999, PhRvL, 83, 3198
Hubbard, A., & Brandenburg, A. 2012, ApJ, 748, 51
Kahniashvili, T., Tevzadze, A. G., Brandenburg, A., & Neronov, A. 2013, PhRvD, 87, 083007
Kerr, R. M., & Brandenburg, A., 1999, PhRvL, 83, 1155
Kleeorin, N., & Rogachevskii, I., 1999, PhRvE, 59, 6724
Kleeorin, N., Moss, D., Rogachevskii, I., & Sokoloff, D. 2000, A&A, 361, L5
Kolmogorov, A.N., 1941, Dokl. A N SSSR, 30, 299
Krause, F., & Rädler, K.-H. 1980, Mean-field Magnetohydrodynamics and Dynamo Theory (Oxford: Pergamon Press)
Losada, I. R., Brandenburg, A., Kleeorin, N., & Rogachevskii, I. 2013, A&A, 556, A83
Matthaeus, W. H., Goldstein, M. L., & Smith, C. 1982, PhRvL, 48, 1256
Moffatt, H. K. 1969, JFM, 35, 117
Moffatt, H. K., Magnetic field generation in electrically conducting fluids, 1978, Cambridge University Press, Cambridge
Obukhov, A. M., 1941, Dokl. A N SSSR, 32, 22
Pevtsov, A. A., Canfield, R. C., & Metcalf, T. R., 1994, ApJ, 425, L117
Seehafer, N., 1990, SoPh, 125, 219
Seehafer, N. 1996, PhRvE, 53, 1283
Stenflo, J. O., 2012, A&A, 541, A17
Su, J. T., Sakurai, T., Suematsu, Y., Hagino, M., & Liu, Y., 2009, ApJ, 697, L103
Taylor, J. B., 1986, RvMP, 58, 741
Venkatakrishnan, P., & Tiwari, S., 2009, ApJ, 706, L114
Warnecke, J., Brandenburg, A., & Mitra, D. 2011, A&A, 534, A11
Warnecke, J., Brandenburg, A., & Mitra, D. 2012, JSWJC, 2, A11
Woltjer, L., 1958a, PNAS, 44, 489
Woltjer, L., 1958b, PNAS, 44, 833
Yousef, T. A., & Brandenburg, A. 2003, A&A, 407, 7
Zeldovich, Y. B., Ruzmaikin, A. A., & Sokoloff, D. D., 1983, Magnetic fields in astrophysics, New York, Gordon and Breach
Zhang, H., 2010, ApJ, 716, 1493
Zhang, H., Moss, D., Kleeorin, N., Kuzanyan, K., Rogachevskii, I., Sokoloff, D., Gao, Y., & Xu, H., 2012, ApJ, 751, 47